Environ Fluid Mech (2010) 10:369–386
DOI 10.1007/s10652-009-9162-3

ORIGINAL ARTICLE

Alternative depth-averaged models for gravity currents and free shear flows

Marko Princevac · Johannes Bühler · Anton J. Schleiss

Received: 23 March 2009 / Accepted: 9 December 2009 / Published online: 19 January 2010

Abstract Two approaches have traditionally been used to describe the widening rate of jets and plumes: the diffusion concept of Prandtl, and the entrainment principle of Morton, Taylor and Turner. The entrainment concept is based on depth-averaged flow scales, and was later applied to plane gravity currents on an incline by Ellison and Turner [ET]. The two parameterizations are compared here for free shear flows, and gravity currents. It is shown that the diffusion concept is suitable for supercritical gravity currents, and that both approaches agree for subcritical ones. Depth-averaged models are also used for open channel flows, but the depth and velocity scales for the two flows are different. Those of ET are derived from the velocity distribution, whereas the depth of an open channel flow is the vertical extent of the dense liquid phase, and the velocity is derived from its flux. To reconcile the two descriptions, we extended the mass-based flow scales of open channel flows to gravity currents in an earlier contribution. In the present study these scales are outlined, and extended further to axisymmetric and non-buoyant free shear flows. Ratios of the diffusion rates in terms of mass- and velocity-based flow scales, are obtained from available experimental data for free shear flows.

Keywords Top-hat scales · Forced plumes · Gravity currents · Open channel flow · Jets · Plumes

M. Princevac
Department of Mechanical Engineering, University of California at Riverside, Bourns Hall A315, Riverside, CA 92521, USA
e-mail: marko@engr.ucr.edu

J. Bühler (✉)
Institute of Environmental Engineering, ETH Zurich, 8093 Zurich, Switzerland
e-mail: buhler@ifu.baug.ethz.ch

A. J. Schleiss
Ecole Polytechnique Fédérale de Lausanne, Laboratory of Hydraulic Constructions, Station 18, 1015 Lausanne, Switzerland
e-mail: anton.schleiss@epfl.ch

1 Introduction

Jets and wakes in neutral environments have been the subject of many studies for about a century. The width of plane and axisymmetric jets has traditionally been defined as the transverse location, b_u, at which the velocity is one-half of its maximum value u_m. Conversely, the maximum value has been used as the relevant velocity scale. When necessary, the corresponding concentration of a tracer was denoted as c_m and the corresponding half-width as $b_c = \lambda b_u$, where λ is a coefficient. By invoking the concept of self-preservation, the fluxes of momentum and volume were expressed in terms of these velocity scales, and a computed shape function. The rate at which the half-width increases in the flow direction x was estimated by Prandtl [1]. His model implies that the outward drift of turbulent structures advected with the mean flow is proportional to their excess velocity, i.e. that $\mathrm{D}b_u/\mathrm{D}t \propto u_m$ (see also [2] and [3]). For a jet-like flow in calm surroundings, $\mathrm{D}b_u/\mathrm{D}t \propto \mathrm{d}b_u/\mathrm{d}x\ u_m$, which leads to a closure relation $\mathrm{d}b_u/\mathrm{d}x = \text{const}$. A later study by Morton, Taylor and Turner [MTT] [4] focused on jets and plumes in stratified environments, which can arise when wastewater is returned to the aquatic environment, or warm flue gases to the atmosphere. Such flows lack in self-preservation and the authors deemed it too difficult to compute shape functions for the velocity distributions in this case. As a consequence, they assumed Gaussian profiles for all flows. To distinguish the ambient stratification from the density distribution within the flow they also introduced a flow boundary, at which the velocity and density changed from constant internal values to the ones in the ambient fluid. The required top-hat (or depth-average) scales of velocity and width were derived from the fluxes of momentum and volume. The volume flux was also needed to keep track of the changing buoyancy flux, and its streamwise increase was specified by an entrainment velocity at the boundary of the jet. This velocity was assumed to be proportional to the mean flow velocity.

The most striking difference between the diffusion and the entrainment concepts is that with Prandtl's model the spatial widening rate of free shear flows in a calm fluid can be determined without making use of the momentum equation, i.e. without considering whether the flow is buoyant or nonbuoyant. Moreover, the widening rates measured for jets and plumes agree to within the experimental error [5–7]. This good agreement does not necessarily follow from Prandtl's model, and the reasons are not quite clear. Similarly, his model does not distinguish between axisymmetric and plane flows, and the widening rates for both of these flows again agree well [6]. The two approaches are consistent with each other for thermals and puffs, and the spreading rates appear to be about the same for buoyant and nonbuoyant flows of this type as well [8].

Prandtl's diffusion model has been used for jets in co-flows after Abramovich [3] and Patel [9]. An equivalent approach was adopted for other jetlike flows by Chu [10], who examined the dynamics of dominant eddies, and derived a flow width $\tilde{b}$ from the intermittency distribution. The MTT approach has been the one generally used for studies of the dilution of effluents in the aquatic environment [11,12]. A combination of both models was proposed by Jirka [7]. We also noticed that the origin of the diffusion concept appears to be getting lost, Patel [9] already quoted Abramovich [3] as attributing it to Prandtl. The two concepts are compared for plane jets and plumes in Sect. 2.

Bottom-hugging gravity currents can be due to an inflow of cold, saline or turbid water into a water body. The entrainment approach was extended to such flows by Ellison and Turner [ET] [13]. These authors also accounted for the presence of an ambient flow, and distinguished the flow from its environment by deriving the depth and velocity scales from the excess velocity distribution. The effect of the slope on entrainment was accounted for by an entrainment function, which depends on the Richardson number of the flow. The ET scales

have been extensively used to describe gravity and turbidity currents in lakes and marine environments [14–17]. Manins and Sawford [18] used them for a field study on katabatic (downslope) winds in a stratified atmosphere. Gravity driven flows have recently attracted increased attention in connection with climate modeling [19], and sedimentation control in reservoirs [20]. A limitation of ET's entrainment concept, and of later models relying on it, is that the value of the entrainment function is the same for wall jets and wall plumes, which does not agree with experimental data. In Sect. 3 we show that this difficulty can be overcome by adopting Prandtl's approach for supercritical gravity currents.

Depth-averaged descriptions similar to those of ET's are also used for open channel flows [21], but their depth scale is the vertical extent of the dense liquid phase, regardless of the velocity distribution. To retain the same type of flow scales for both types of flows, Bühler and Siegenthaler [22] extended these latter scales to gravity currents. Princevac et al. [23] modified the underlying concepts and considered non-Boussinesq flows as well as ambient co-flows. The results are outlined in Sect. 4.

Mass-based flow scales are then further extended to free shear flows in Sect. 5, and experimental data for plane and axisymmetric jets and plumes are reanalyzed in terms of these scales. Conclusions are drawn in the final section.

2 Relation between the diffusion and entrainment concepts

Prandtl [1] proposed a model for the widening rate of weak jets in an ambient coflow of velocity u_a. He assumed that the transverse drift of turbulent structures carried along in such a nearly self-preserving flow is proportional to the characteristic transverse velocity fluctuations v', which leads to

$$\frac{\mathrm{D}b_\mathrm{u}}{\mathrm{D}t} = v' \tag{1}$$

where b_u is the half-width based on the excess velocity (Fig. 1). According to his old mixing length concept the turbulent shear stress is $\rho\overline{u'v'} = \rho l^2(\partial\bar{u}/\partial y)^2$, where l is the mixing length, ρ the fluid density, $\bar{u}$ the local flow velocity, y the transverse coordinate, and the overbars denote time-averaged quantities. As the transverse fluctuations are proportional to the streamwise ones, this leads to a closure relation

$$\frac{\mathrm{D}b_\mathrm{u}}{\mathrm{D}t} \propto l\frac{\partial\bar{u}}{\partial y} \propto \frac{lu_\mathrm{em}}{b_\mathrm{u}} \propto \alpha u_\mathrm{em}, \tag{2}$$

where α is the constant ratio of the mixing length and the jet width, and u_em the maximum excess velocity. Similarity arguments then imply that the mean values of the lateral drift v_d of the turbulent structures, and of their excess velocity u_es, are proportional to each other (Fig. 1).

The fact that the excess velocity distributions are similar for most free shear flows also agrees with the evidence that the widening rate is fairly universal. Prandtl [24] later assumed that $\overline{u'v'} = \pm\kappa b_\mathrm{u}u_\mathrm{em}\partial\bar{u}/\partial y$, i.e. that the kinematic eddy viscosity $\kappa b_\mathrm{u}u_\mathrm{em}$ is constant in a cross-section (see also [2]). The profile function then agrees with that of laminar jets, and this approach leads to the same dependence as (2), since $v' \propto \kappa^{1/2}u_\mathrm{em}$; see also [3] and [25].

The flow scales of MTT were extended by ET to gravity currents by allowing for ambient coflows of velocity u_a. They derived top-hat scales for the depth H, and the characteristic excess velocity U of plane flows according to

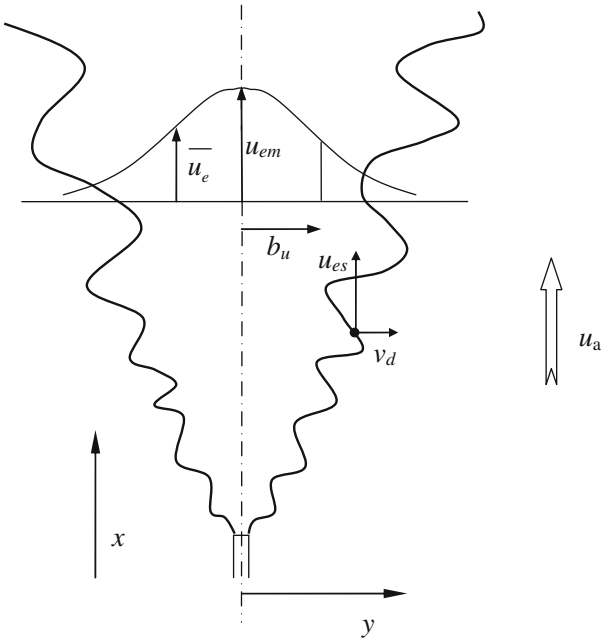

Fig. 1 Jet in a co-flow. Half-width b_u, maximum excess velocity u_{em}. Prandtl's model implies that the mean values of the transverse drift v_d of large structures, and of their excess velocity u_{es} are proportional to each other

$$\begin{aligned} UH &= \int (\bar{u} - u_a)\,dy \\ U^2H &= \int (\bar{u} - u_a)^2 dy \end{aligned} \tag{3}$$

For free shear flows H is the top-hat half-width, and the integration is carried from the center-plane to a location in the ambient fluid at which the velocity gradient $d\bar{u}/dy$, and the velocity fluctuations can be neglected.

They stated the entrainment relation as

$$\frac{d}{dx}\left[(U + u_a)H\right] = EU \tag{4}$$

where E is an entrainment function, to be specified, which assumes constant values E_j and E_p for jets and plumes ($u_a = 0$).

Prandtl's diffusion relation can also be restated in terms of top-hat scales. In the spirit of Patel [9] and [26] the corresponding relation can be stated as

$$\frac{dH}{dx} = D\frac{cU}{cU + u_a} \tag{5}$$

where D is a diffusion function and c a constant, which has no effect when $u_a = 0$. The value of c depends on the excess velocity of the structures which define the width scale H. According to Patel [9], Prandtl assumed a value of $u_{em}/2$ for this velocity, which leads to $c = 1/\sqrt{2}$ for a Gaussian profile. Patel himself proposed a velocity u_{em} instead, which leads to $c = \sqrt{2}$, and claimed better agreement with experimental data. In terms of the depth-averaged model used here, we shall adopt the intermediate value $c = 1$, which implies that the structures which define the width of the flow travel at a velocity $U + u_a$. As the velocity

profiles are approximately Gaussian for both jets and plumes, the widening rates D_j and D_p can again be expected to agree well.

To compare E and D we consider a thin slab of fluid of width H and thickness δ which is advected with the velocity $U + u_a$ in terms of the depth-averaged description. When $\mathrm{d}u_a/\mathrm{d}x = 0$, $\mathrm{D}\delta/\mathrm{Dt} \cong \mathrm{d}U/\mathrm{d}x\ \delta$, and the rate of change $\mathrm{D}(H\delta)/\mathrm{Dt}$ of the slab volume can be expressed in the Eulerian frame of reference as

$$\frac{\mathrm{d}H}{\mathrm{d}x}(U + u_a)\delta + H\frac{\mathrm{d}U}{\mathrm{d}x}\delta - \mathrm{E}U\delta \cong 0 \tag{6}$$

The term $\mathrm{d}H/\mathrm{d}x\ (U + u_a)\ \delta$ is the rate at which the slab volume grows in time as the slab widens, the term $H\ \mathrm{d}U/\mathrm{d}x\ \delta$ is the growth in case it thickens, and the rate $\mathrm{E}U\delta$ is the resulting horizontal inflow of ambient fluid through its outer surface. By omitting δ, and with the widening rate in time $\mathrm{d}H/\mathrm{d}x\ (U + u_a) = \mathrm{D}U$ according to (5), this can also be written as

$$\frac{\mathrm{d}H}{\mathrm{d}x}(U + u_a) + H\frac{\mathrm{d}U}{\mathrm{d}x} = \mathrm{D}U\left(1 + \frac{H}{\mathrm{D}U}\frac{\mathrm{d}U}{\mathrm{d}x}\right) = \mathrm{E}U \tag{7}$$

The diffusion model thus specifies the temporal widening rate $\mathrm{d}H/\mathrm{d}x\ (U + u_a)$ in terms of the excess velocity as $\mathrm{D}U$. Conversely, the entrainment rate $\mathrm{E}U$ also depends on the velocity gradient, which is determined by the momentum equation of the flow. Note that $\mathrm{E}U$ is the velocity of ambient fluid through the rim of the widening slab. We shall see that it is not necessarily equal to the entrainment velocity, i.e. the transverse motion of the ambient fluid. For pure plumes U is constant [6], and the gradient vanishes, such that the spreading coefficient D_p for plumes corresponds to the corresponding entrainment coefficient E_p for these flows. The velocity in jets, however, varies with $x^{-1/2}$ [6], and by noting that $H = \mathrm{D}x$, the expression in the second parenthesis is 1/2. E_j is then $D_j/2 = E_p/2$ provided that the corresponding diffusion coefficients D_j and D_p for jets and plumes are assigned the same value, as proposed by List and Imberger [5], Chu [10], and other investigators. The transition from the value of 1/2 to 1 of this term along a forced plume (i.e. a buoyant jet) has been related to the Richardson or Froude number of the flow when the MTT entrainment relation is used [11]. Chu [10] devised a spread model for dominant eddies in the flow, which is similar to that of Prandtl, and derived the ratios of E and the widening rate for plane and axisymmetric jets and plumes.

The difference between plane plumes and jets is illustrated in Fig. 2 by adopting ET's highly idealized depth averaged description. On the left, a thin fluid slab in the plume is shown at two different heights and times. In such flows the velocity $U(x)$ remains constant, such that the widening rate $\mathrm{d}H/\mathrm{d}x\ U = D_pU$ of the slab is due to the inflow $-E_pU$ through its outer surface, marked by cross-hatching (new fluid). This implies that the water particles move downstream within the slab after entering into it, and maintain their lateral position y during their onward journey (old fluid).

The situation is different for jets, which are decelerating due to entrainment, i.e. the mass flux carrying the available momentum is increasing in the flow direction. As a result of the deceleration, the term in $\mathrm{d}U/\mathrm{d}x$ is negative, and the slab is thinning, such that the particles contained in it keep moving outwards. Due to this outward motion, the inflow velocity through the rim of the slab is only half as great as for a plume for the same value of U. In other words, the spatial widening rate is due in about equal parts to the thinning of the slab, and the inflow of new particles. It can be shown along the same lines that 5/6 and 1/2 of the spread $\mathrm{d}B/\mathrm{d}x$ is due to inflow for an axisymmetric plumes and jets of radius B, respectively, in accordance with [10] and other authors.

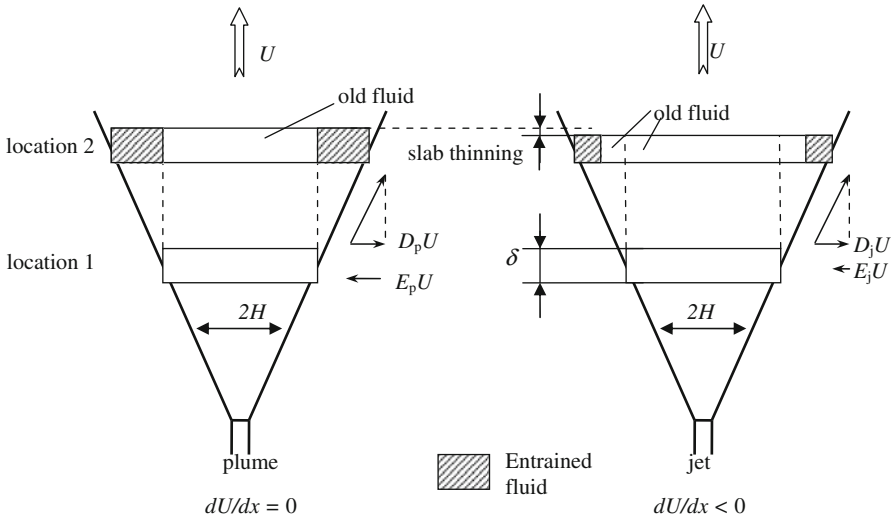

Fig. 2 Depth-averaged view of a slab of fluid of thickness δ at two different downstream positions in a plane plume and a plane jet. The streamwise velocity in the jet decreases, and the slab becomes thinner. The entrainment of new fluid (cross-hatched) is thus only half as great for the jet as for the plume, whereas the two widening rates D_j and D_p agree closely

When a jet enters into a co-flow, the excess velocity u_{em} keeps decreasing, and the flow becomes approximately self-preserving in the range $U \ll u_a$. The excess flux of momentum of the jet in that region is $m_e = 2HUu_a$, and constant. H and U can then be evaluated from (7) as $H = (D_{jc}m_e x/u_a^2)^{1/2}$, and $U = [m_e/(4D_{jc}x)]^{1/2}$, with D_{jc} denoting the diffusion coefficient in co-flows. The widening rate $\mathrm{d}H/\mathrm{d}x\ u_a = D_{jc}\,U$ in (7) is thus proportional to $x^{-1/2}$, and the thinning term $H\ \mathrm{d}U/\mathrm{d}x$ to x^{-1}. The thinning term thus decreases faster, and the internal flow becomes similar to that in a plume, in which this term vanishes. The inflow velocity $-E_{jc}U$ through the rim of the moving slab is then again opposite, and nearly equal, to its outward velocity $D_{jc}U$ due to diffusion. Since $U \ll u_a$, the streamwise velocity u_a of the inflowing external fluid is close to that within the jet, and the inflow through the rim of the slab is horizontal, as it is for jets and plumes in calm fluids. For jets in a co-flow, however, the transverse motion of the external fluid towards the jet, i.e. the entrainment velocity, vanishes, and the excess volume flux HU remains constant. In the Eulerian frame of reference the inflow velocity into the jet is u_a, and parallel to the centerplane of the flow (Fig. 1). A few attempts have been made to quantify the corresponding increase $\mathrm{d}H/\mathrm{d}x\ u_a$ of the volume flux due to diffusion [11,26]. The lack of a transverse motion of the ambient fluid towards the jet, and the different directions of the inflow in the Eulerian and the Lagrangian frame of reference, may have contributed to past discussions about what entrainment is [27]. Similar to jets in a co-flow, thermals and puffs also grow in time due to turbulent outward diffusion of their boundary. There is no net ambient flow towards these clouds, and no entrainment velocity, because there is no sink of mass within them [8].

The entrainment rate EU of external fluid into a free jet or plume also corresponds to the small-scale entrainment of new fluid through the highly contorted turbulent/nonturbulent interface of these flows. The corresponding small-scale entrainment velocity corresponds to the diffusion of vorticity and tracer into the irrotational outer fluid, and Holzner et al. [28] showed that it essentially scales with the Kolmogorov velocity. This implies that ratio of the

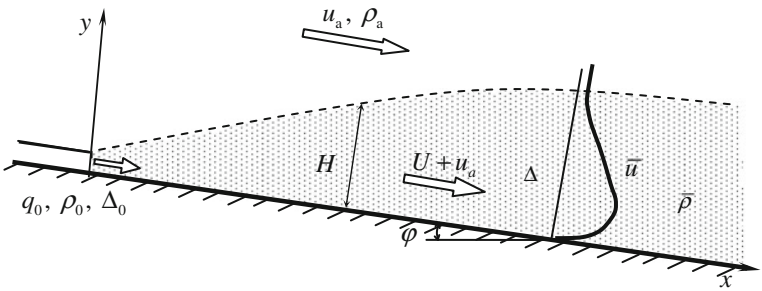

Fig. 3 Definition sketch for a developing gravity current in unstratified and deep water. ET's top-hat scales for depth H, excess velocity U, and buoyancy Δ are based on the distribution of the excess velocity $\bar{u} - u_a$, and on the buoyancy flux. q_0 is the initial discharge, per unit width

area of the small-scale interface per unit top-hat interface depends on the Reynolds number of the flow [29]. The above considerations on EU in (7) indicate that the ratio depends not only on the local excess velocity U, and the Reynolds number, but also on the streamwise velocity gradient dU/dx, i.e. on the momentum equation of the flow under consideration. An additional difficulty is that the small-scale entrainment velocity has a viscous as well as an inviscid component [30].

In the following section, the above comparison of the entrainment and diffusion concepts is extended to gravity currents.

3 Diffusion model for gravity currents

Gravity currents in a deep and unstratified upper layer were investigated by ET. The flow, sketched in Fig. 3, is generally not self-preserving as it develops, and ET modified MTT's approach to describe them.

The depth H and the velocity U in their entrainment relation (4) were derived from the velocity distribution as stated in (3). The buoyancy scale Δ was related to the buoyancy flux j by

$$(U + u_a)\,\Delta H = j = g \int \frac{(\bar{\rho} - \rho_a)\bar{u} + \overline{\rho' u'}}{\rho_a} \mathrm{d}y = \frac{g}{R} \int \frac{(\bar{\rho} - \rho_a)\bar{u}}{\rho_a} \mathrm{d}y \tag{8}$$

where R is the ratio of the mean and total buoyancy flux. ET neglected the turbulent contribution to the flux, but in their experiments they also determined Δ from the mean velocity distribution and the initial buoyancy flux $j_0 = \Delta_0 q_0$. It is desirable to retain the turbulent contribution whenever possible, as the total buoyancy flux it is the only flux which can be truly conserved. Their shallow water equations for a dilute gravity current in a calm environment are

$$\frac{\mathrm{d}y}{\mathrm{d}x}(UH) = \mathrm{E}U \tag{9}$$

$$\frac{\mathrm{d}}{\mathrm{d}x}\left(U^2 H + \frac{S_1}{2}\Delta H^2 \cos\varphi\right) = S_2 \Delta H \sin\varphi - C_\mathrm{D} U^2 \tag{10}$$

$$\frac{\mathrm{d}}{\mathrm{d}x}(\Delta U H) = 0. \tag{11}$$

φ is the slope angle, $\mathrm{E}(Ri)$ is an entrainment function, which depends on the Richardson number $Ri = \Delta H \cos\varphi / U^2$, and C_D is a Chezy-type drag coefficient.

The shape factors S_1 and S_2 relate the excess bottom pressure and the excess pressure force to the flow scales, i.e.

$$\begin{aligned} S_1 \Delta H^2 &= 2g \int \frac{(\bar{\rho} - \rho_\mathrm{a})}{\rho_\mathrm{a}} y \mathrm{d}y \\ S_2 \Delta H &= g \int \frac{(\bar{\rho} - \rho_\mathrm{a})}{\rho_\mathrm{a}} \mathrm{d}y \end{aligned} \tag{12}$$

By making use of (9)–(11), the variation of the depth and the Richardson number was expressed as

$$\frac{\mathrm{d}H}{\mathrm{d}x} = \frac{\mathrm{E}\left(2 - \frac{S_1}{2} Ri\right) - S_2 Ri \tan\varphi + C_\mathrm{D}}{1 - S_1 Ri} \tag{13}$$

$$\frac{H}{3Ri} \frac{\mathrm{d}Ri}{\mathrm{d}x} = \frac{\mathrm{E}\left(1 + \frac{S_1}{2} Ri\right) - S_2 Ri \tan\varphi + C_\mathrm{D}}{1 - S_1 Ri} \tag{14}$$

One feature of (13) and (14) is that the denominator vanishes when $Ri = 1/S_1$, which is of order one. The flow is critical under these conditions, in analogy to open channel flows. An important result of ET is that on a constant slope Ri and $\mathrm{d}H/\mathrm{d}x$ vary along the flow depending on the source conditions, and finally adjust to a constant value. In this final equilibrium state the flow is called uniform, and the velocity is constant, as it is in free plumes.

Wall jets, and plumes on a vertical wall, are special cases of gravity currents, as the Richardson number $Ri = \Delta H \cos\varphi / U^2$ vanishes for both of these flows. As an estimate for E for wall jets, ET adopted a value of 0.075 for free jets, corresponding to $\mathrm{d}H/\mathrm{d}x = 2E_\mathrm{j} = 0.15$ [31]. They already noted that the values for free plumes, for which Ri also vanishes, appeared to be higher, but thought that insufficient data were available to make definite conclusions. More recent experiments by Patel [9] indicate that their spreading rate $\mathrm{d}H/\mathrm{d}x$ of wall jets is about 0.091 (with $C = 0.065$). Similar to what is found for free shear flows, this is again in excellent agreement with the value $\mathrm{d}H/\mathrm{d}x = 0.095 \pm 0.005$ of Grella and Faeth [32] for wall plumes, which have a similar velocity distribution. Based on these considerations it is tempting to adopt a diffusion relation

$$\frac{\mathrm{d}H}{\mathrm{d}x} = \mathrm{D} \tag{15}$$

based on (5) to specify the widening rate of gravity currents. ET and later investigators [17] determined the entrainment relation $\mathrm{E}(Ri)$ for equilibrium flows ($\mathrm{d}U/\mathrm{d}x = 0$), such that the two descriptions are identical for that case according to (7), i.e. $\mathrm{D}(Ri) \equiv \mathrm{E}(Ri)$. Relation (15) thus describes the transition from a forced wall plume to a wall plume if the value of D at $Ri = 0$ is increased slightly from 0.075 to about 0.093. The relation can, however, also be applied to other slopes, as it becomes equivalent to (9) with $\mathrm{E} = \mathrm{D}$ as soon as the equilibrium state is reached. By applying (15) to the momentum and buoyancy equations (10) and (11), the variation of the Richardson number can be stated as

$$\frac{H}{3Ri} \frac{\mathrm{d}Ri}{\mathrm{d}x} = \frac{\mathrm{D}\left(1 + \frac{S_1}{2} Ri\right) - S_2 Ri \tan\varphi + C_\mathrm{D}}{2 - \frac{S_1}{2} Ri} \tag{16}$$

whereas the nominator of this relation agrees with that in (14) for $\mathrm{E} = \mathrm{D}$, the denominators are quite different. In particular, the one in (16) no longer vanishes when gravity currents are

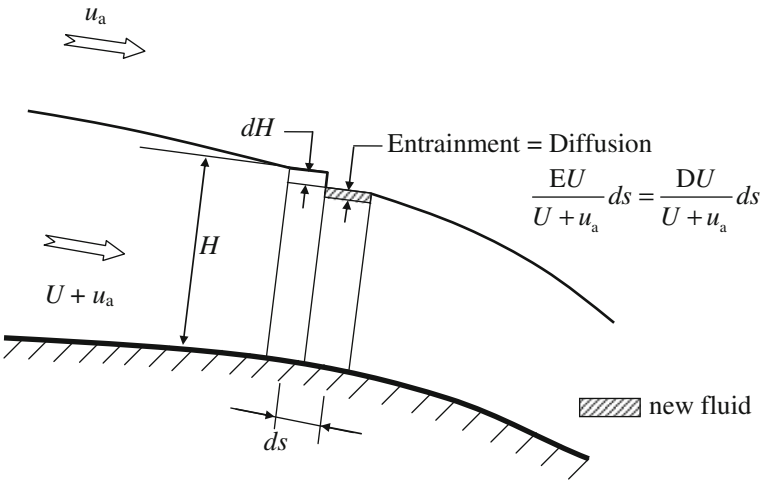

Fig. 4 Depth-averaged view of subcritical gravity current with small entrainment. The widening rate due to entrainment is equal to the one due to diffusion, such that E ≡ D, see (5), (17)

critical, and the Richardson number is close to one, but when it is close to 4. The reason is that only (9), but not (15) is consistent with the continuity equation for open channel flows. Expressions (15) and (16) are thus appropriate for developing supercritical flows, but not for small slopes, on which the resulting equilibrium flow can be subcritical.

To evaluate numerical models for gravity currents, Odier et al. [33] performed measurements in flows on a steep slope (10°), for which the diffusion model applies. They found that the mixing length concept provides a better description of the turbulent fluxes $\overline{u'v'}$ and $\overline{\rho'v'}$ than a constant eddy viscosity does.

On mild slopes the entrainment is small, and any changes of the last two terms in the nominator of (14) become dominant. The streamwise velocity gradient is then primarily due to changes in slope, roughness and topography, and the volume flux is essentially conserved except for a thin, superimposed layer of ambient fluid (Fig. 4).

When u_a remains constant, the continuity equation (4) can be restated for this case as

$$\frac{dH}{ds} = E\frac{U}{U+u_a} - \frac{H}{(U+u_a)}\frac{dU}{ds}, \tag{17}$$

where s is the streamwise coordinate. As noted earlier, E = D for uniform flows ($dU/ds = 0$), and the first term on the RHS corresponds to the diffusion relation (5) with $c = 1$. As the entrainment is small, the second term on the RHS of (17) is essentially unrelated to the first one, and represents any depth change due to variations in slope or roughness. Even for nonuniform subcritical flows the entrainment relation (4) can thus be restated in terms of D as

$$\frac{d}{dx}[(U+u_a)H] = DU \tag{18}$$

Similarly, E can be replaced by D in (13) and (14) for these flows. Prandtl's concept, and the diffusion relation, thus accounts for that part of the depth change which is due to fluid entrainment in both supercritical and subcritical gravity currents.

4 Mass-based flow scales

As mentioned in Sect. 1, another relevant aspect of ET's shallow water equations is that the flow scales H and U in (3) disagree from the depth and velocity scales of open channel flows because they are derived from the velocity distribution instead of the excess mass distribution. Similarly, the buoyancy scale Δ in (8) is derived by dividing the buoyancy flux by the volume flux. Δ is thus a quantity related to the transport of buoyancy, and the mean concentration $\Delta/\Delta_0 = q_0/(U + u_\mathrm{a})H$ of effluent in a flow is unrelated to the buoyancy distribution.

Bühler et al. [34], and Princevac et al. [23] reconciled the flow scales for open channel flows with those of gravity currents in a co-flow by setting

$$\begin{aligned} g'h^2 &= \frac{2g\int(\bar{\rho}-\rho_a)y\mathrm{d}y}{\rho_0} = S_1\Delta H^2 \\ g'h &= \frac{g\int(\bar{\rho}-\rho_a)\mathrm{d}y}{\rho_0} = S_2\Delta H \\ g'hu &= \frac{g\int\left((\bar{\rho}-\rho_a)\bar{u}+\overline{\rho'u'}\right)\mathrm{d}y}{\rho_0} = (U+u_\mathrm{a})\Delta H = j_0 \end{aligned} \tag{19}$$

The two quantities associated with shape constants S_1 and S_2 by ET are thus used to define the flow scales g' and h, whereas the buoyancy flux now determines the flow velocity u. The excess velocity u_e and the excess buoyancy flux $g'hu_\mathrm{e}$ can be expressed as

$$g'hu_\mathrm{e} = \frac{g\int\left((\bar{\rho}-\rho_a)(\bar{u}-u_a)+\overline{\rho'u'}\right)\mathrm{d}y}{\rho_0} = j_0 - g'hu_\mathrm{a} = [U+(1-S_2)u_\mathrm{a}]\,\Delta H \tag{20}$$

The fluid density, or the concentration of a stratifying agent, is a scalar quantity, and generally easier to measure than velocity. At least in laboratory experiments, the concentration can also be made to vanish outside the flow. When the buoyancy flux is known, and conserved, u can be obtained without carrying out velocity measurements. This also holds for the excess velocity u_e when the ambient velocity is known, and constant in the transverse direction. The option of deriving u instead of Δ from the flux of buoyancy also allows for a simple distinction of the excess buoyancy flux $g'hu_\mathrm{e}$, which depends on both the excess velocity and buoyancy distributions, from the flux $g'hu_\mathrm{a}$ associated with the ambient velocity, which only depends on the buoyancy distribution. This is relevant for developing flows, in which the ratio of the two fluxes changes in the streamwise direction. As S_1 and S_2, link the two profiles, this leads to a variation of these shape factors along the flow even in case the profiles remain similar.

Shape factors β and γ were introduced to relate the excess fluxes of volume and momentum to these flow scales as

$$\gamma h(u-u_\mathrm{a}) = HU, \quad \gamma(\beta u - u_\mathrm{a})uh = (U+U_\mathrm{a})UH \tag{21}$$

where γ modifies the depth h (Fig. 5).

The scales derived in (19) are consistent with the ones for open channel flows, where ρ_a and u_a are generally neglected, such that $\rho = \rho_0$. As the density is known, $g' = g$, and the bottom pressure $\rho_0 gh$ alone is required to derive a depth scale h. Similarly, γ in (21) is equal to 1, and β is the momentum coefficient, or Boussinesq coefficient, for open channel flows, which accounts for nonuniformities of the velocity distribution [21].

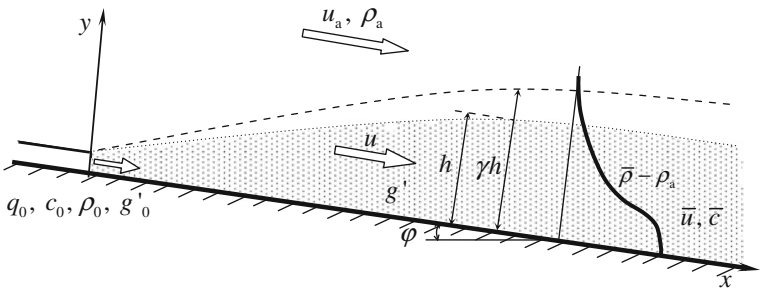

Fig. 5 Definition sketch for mass-based flow scales of depth h, buoyancy g' and velocity u, which are derived from the excess density distribution $\bar{\rho} - \rho_a$, and the buoyancy flux. The excess volume flux is confined to the depth γh

The corresponding relations for non-Boussinesq flows, which are intermediate between dilute gravity currents and open channel flows, were derived by Princevac et al. [23]. These authors also evaluated available experimental and field data [16,35], and showed that γh exceeds the mass-based depth h in gravity currents (Fig. 5). The bottom layer, of velocity u, is thus considered as consisting of dense fluid of depth h, and of superimposed ambient fluid of depth $(\gamma - 1)h$. γ was found to be in the range from 1.0 to 2.7. β again accounts for nonuniformities of the velocity distribution, and is in about the same range from 1.03 to 1.33 as for open channel and ducted flows [21]. Whereas S_1 and S_2 are difficult to interpret, β is comparable to the corresponding quantity in open channel flows, and γ is the depth ratio of the top-hat heights of the velocity and density distributions, similar to the turbulent Schmidt number $1/\lambda = b_u/b_c$ of free shear flows.

The shallow water equations of ET can be written in terms of fully mass-based scales. For calm ambients ($u_a = 0$) and in terms of (10), (11), and (18), the equations for subcritical flows are

$$\frac{\mathrm{d}}{\mathrm{d}x}(uh) = \mathrm{D}^* u \tag{22}$$

$$\frac{\mathrm{d}}{\mathrm{d}x}(\beta\gamma u^2 h + \frac{1}{2} g' h^2 \cos\varphi) = g' h \sin\varphi - C_\mathrm{D}^* u^2 \tag{23}$$

$$\frac{\mathrm{d}}{\mathrm{d}x}(g' u h) = 0 \tag{24}$$

The star denotes definition in terms of mass-based flow scales. Identities (19), (20) and (21) can be used to derive the relation between the two sets of scales. For calm environments $h = HS_1/S_2$, $g' = \Delta S_2^2/S_1$, $u = U/S_2$, $\beta = S_2$, $\gamma = S_2^2/S_1$, $\mathrm{D}^* = \mathrm{D}S_1/S_2$, and $C_\mathrm{D}^* = C_\mathrm{D} S_2^2$. ET reported values of S_1 from 0.2 to 0.3, and of S_2 from 0.6 to 0.9. When the buoyancy flux is known, uncertainties related to velocity measurements thus affect the shape factors in the momentum equation (23) only, but not the flow scales. Princevac et al. [23] derived the shallow water equations by considering ambient co-flows, and derived the corresponding relations between the flow parameters in the mass-based and velocity based descriptions.

Relations (22)–(24) can be expressed as

$$\frac{\mathrm{d}h}{\mathrm{d}x} = \frac{\mathrm{D}^*\left(2\beta\gamma - \frac{1}{2}Ri^*\right) - Ri^*\tan\varphi + C_\mathrm{D}^*}{\beta\gamma - Ri^*} \tag{25}$$

$$\frac{h}{3Ri^*}\frac{\mathrm{d}Ri^*}{\mathrm{d}x} = \frac{\mathrm{D}^*\left(\beta\gamma + \frac{1}{2}Ri^*\right) - Ri^*\tan\varphi + C_\mathrm{D}^*}{\beta\gamma - Ri^*} \tag{26}$$

As it does in (14), the denominator again vanishes when $Ri^* = g'h\cos\varphi/u^2 \approx 1$.

Relations to (15), (10) and (11) for supercritical flows can similarly be restated in terms of mass-based scales as

$$\frac{\mathrm{d}h}{\mathrm{d}x} = \mathrm{D}^* \tag{27}$$

$$\frac{h}{3Ri^*}\frac{\mathrm{d}Ri^*}{\mathrm{d}x} = \frac{\mathrm{D}^*\left(\beta\gamma + \frac{1}{2}Ri^*\right) - Ri^*\tan\varphi + C_\mathrm{D}^*}{2\beta\gamma - \frac{1}{2}Ri^*} \tag{28}$$

The denominators in (26) and (28) again differ, as they do in (14) and (16).

A set of slightly different, and intermediate, flow scales was proposed by Noh and Fernando [36]. They also derived the velocity scale by dividing the buoyancy flux by the excess bottom pressure, but distinguished only a single depth $\mathrm{h_i} = \gamma h$. They retained ET's concept of dilution, and their buoyancy scale is ratio of the buoyancy flux $g'hu$ and the flux γhu of volume, such that $\mathrm{g_i'} = g'/\gamma$. Intermediate flow scales are related to fully mass-based ones by $\mathrm{u_i} = u$, $\mathrm{Ri_i} = Ri^*$, $\gamma_i = \gamma$, $\mathrm{D_i} = \gamma\mathrm{D}^*$, and $\beta_i = \beta$.

Mass-based width scales can also be derived from the concentration distribution $\bar{c}$ of a tracer, which is added to the discharge. This technique has been used in flow visualizations to determine the visible width of unsteady flows, such as thermals and puffs. Similarly, (19) can be expressed in terms of $\bar{c}$ instead of the excess density to derive flow scales u and h and c for nonbuoyant jets. A width scale $\tilde{b}$ based on the intermittency distribution was proposed for jet-like flows by Chu [10]. Scales based on the vorticity, or tracer distribution, are also suitable for more complex flows, in which the distribution of the streamwise velocity ceases to be relevant. An example are jets in a cross-flow, where the streamwise excess velocity gradually vanishes in the bent-over region, and the transverse excess velocity becomes dominant [37]. Prandtl's model specifies the outward drift of turbulent structures as they are advected downstream with the main flow, and the large-scale transverse diffusion of tracer and turbulence associated with this process. Mass-based flow scales are, therefore, well suited for the description of this diffusion process.

Whereas the identity $\mathrm{E}(Ri) = \mathrm{D}(Ri)$ allows a specification of $\mathrm{D}(Ri)$ based on previous work, we do not have sufficient information to provide the relations $\mathrm{D}^*(Ri^*)$ and $\gamma(Ri^*)$ for the entire range of gravity currents. In a first step we shall evaluate the widening rates D^* for free shear flows in the next section, and compare them with the corresponding values of D.

5 Jets and plumes

Mass-based flow scales for gravity currents outlined in (19) can also be used for plane plumes. Equivalent scales for jets can be derived from the concentration $\bar{c}$ of a passive tracer contained in the flow, even though the scales then no longer reflect gravity forces. To remain consistent with the notation for gravity currents, H and h will denote one-half of the flow width, q_0, m_0 and j_0 one-half the initial fluxes of volume, momentum and buoyancy.

The non-uniformity of the excess velocity distribution is the one relevant for the excess momentum flux. This flux can then be suitably expressed as

$$m_e = \gamma h u_e(\beta_e u_e + u_a) = \int_0^\infty \bar{u}(\bar{u} - u_a)\mathrm{d}y = HU(U + u_a), \tag{29}$$

where $\gamma h u_e$ is the excess volume flux, and the momentum coefficient β_e based on the excess velocity is

$$\gamma \beta_e u_e^2 h = \int_0^\infty (\bar{u} - u_a)^2 \mathrm{d}y = HU^2 \tag{30}$$

Analogous scales can be defined for axisymmetric flows. In terms of the concentration of a tracer they correspond to

$$\begin{aligned}
\pi b^3 c &= \frac{3\pi}{4}\int_0^\infty \bar{c} r^2 \mathrm{d}r = S_1 \pi B^3 C, \\
\pi b^2 c &= 2\pi \int_0^\infty \bar{c} r \mathrm{d}r = S_2 \pi B^2 C \\
\pi b^2 c u &= c_0 Q_0 = \frac{1}{R} 2\pi \int_0^\infty \bar{c}\bar{u} r \mathrm{d}r = \pi B^2 C(U + u_a) \\
\gamma \pi b^2 u_e &= 2\pi \int_0^\infty (\bar{u} - u_a) r \mathrm{d}r = \pi B^2 U \\
\gamma \beta_e \pi b^2 u_e^2 &= 2\pi \int_0^\infty (\bar{u} - u_a)^2 r \mathrm{d}r = \pi B^2 U^2
\end{aligned} \tag{31}$$

where r is the radial distance, and caps are again used to denote velocity-based scales.

By following the approach of Wright [38] the widening rates are expressed as

$$\frac{\mathrm{d}B}{\mathrm{d}x} = \mathrm{D}\frac{U}{U + u_a}, \quad \frac{\mathrm{d}b}{\mathrm{d}x} = \mathrm{D}^* \frac{u_e}{u} \tag{32}$$

In comparing the top-hat widths of plane and axisymmetric flows it should be noted that they are different when the half-width b_u is equal in both types of flows. For Gaussian profiles it can be shown that $B/H = 1.13$ in this case. Similarly, $b/h = 1.18$ for a given b_c.

Data on jets and plumes, evaluated from recent recommendations, are presented in Tables 1 and 2. Axisymmetric flows are from a source of total strength Q_0, M_0 and J_0. All authors assumed Gaussian profiles, and the width scale b_g is the one at which the velocity has decayed to $\mathrm{e}^{-1} u_{em}$. Velocities $\boldsymbol{U}$ and $\boldsymbol{u}$ and concentrations $\boldsymbol{C}$ and $\boldsymbol{c}$ are made dimensionless in the same way as u_m, and c_m for plane and axisymmetric flows.

The last rows (Min/Max) show the ratio of the minimum and maximum values of the basic flow scales in a given column, and provides a measure for their consistency. The recommendations by Jirka [7,12], as well as those by Lee and Chu [6] are intended for dilution models, and the flow scales are adjusted to include the turbulent buoyancy flux, such that $R = 1$. The

Table 1 Plane flows

Author	Jet				Plume			
	$\frac{b_g}{x}$	λ	$\boldsymbol{u}_m = u_m\left(\frac{x}{2m_0}\right)^{1/2}$	$\boldsymbol{c}_m = \frac{c_m(2m_0x)^{1/2}}{2c_0q_0}$	$\frac{b_g}{x}$	λ	$\boldsymbol{u}_m = \frac{u_m}{2j_0^{1/3}}$	$\boldsymbol{c}_m = \frac{c_m(2j_0)^{1/3}x}{2c_0q_0}$
Jirka [12]	0.14	1.3	2.38[a]	2.13	0.14	1.3	2.10	2.38
Lee and Chu [6]	0.12	1.35	2.58	2.27	0.116	1.35	2.26	2.68
Hossain and Rodi [39]	0.132	1.29	2.40	2.00	0.144	1.08	1.90	2.40
Fisher et al. [11]	0.116	1.35	2.41	2.38	0.116	1.35	1.66	2.38

Jet Author	H/x = D	h/x = D*	$\gamma h/x$	$\boldsymbol{U}$	$\boldsymbol{u}$	$\boldsymbol{C}$	$\boldsymbol{c}$	R	S_1	$S_2 = \beta$	γ
Jirka [12]	0.175	0.205	0.20	1.68	1.45	1.69	1.67	1.00	1.36	1.16	0.99
Lee and Chu [6]	0.150	0.183	0.18	1.82	1.54	1.82	1.78	1.00	1.44	1.19	0.98
Hossain and Rodi [39]	0.165	0.192	0.17	1.70	1.66	1.78	1.57	0.89	1.19	1.02	0.88
Fisher et al. [11]	0.145	0.177	0.16	1.70	1.51	2.02	1.87	0.95	1.37	1.13	0.93
Min/Max	0.829	0.860		0.92	0.88	0.837	0.840				

Plume Author	H/x=D	h/x=D*	$\gamma h/x$	$\boldsymbol{U}$	$\boldsymbol{u}$	$\boldsymbol{C}$	$\boldsymbol{c}$	R	S_1	$S_2 = \beta$	γ	$\frac{\Delta H}{U^2}$	$\frac{g'h}{u^2}$
Jirka [12]	0.175	0.205	0.20	1.48	1.28	1.89	1.87	1.00	1.36	1.16	0.99	0.15	0.24
Lee and Chu [6]	0.145	0.177	0.17	1.60	1.35	2.15	2.10	1.00	1.44	1.19	0.98	0.12	0.21
Hossain and Rodi [39]	0.180	0.175	0.16	1.34	1.51	2.06	1.88	0.85	0.86	0.89	0.91	0.21	0.14
Fisher et al. [11]	0.145	0.177	0.11	1.17	1.51	2.93	1.87	0.65	0.94	0.78	0.64	0.31	0.14
Min/Max	0.806	0.855		0.73	0.85	0.64	0.89						

[a] From the entrainment coefficient

Table 2 Axisymmetric flows

Author	Jet				Plume			
	$\frac{b_g}{x}$	λ	$\boldsymbol{u}_m = \frac{u_m x}{M_0^{1/2}}$	$\boldsymbol{c}_m = \frac{c_m M_0^{1/2} x}{c_0 Q_0}$	$\frac{b_g}{x}$	λ	$\boldsymbol{u}_m = \frac{u_m x^{1/3}}{J_0^{1/3}}$	$\boldsymbol{c}_m = \frac{c_m J_0^{1/3} x^{5/3}}{c_0 Q_0}$
Jirka [7]	0.11	1.2	7.25	6.17	0.10	1.2	4.9	11.11
Lee, Chu [6]	0.114	1.2	7.0	5.94	0.105	1.19	4.71	10.46
Hossain, Rodi [39]	0.103	1.31	7.0	5.64	0.135	0.93	3.79	10.98
Fisher et al. [11]	0.107	1.187	7.0	5.6	0.10	1.2	4.7	9.1

Jet Author	$B/x = \mathrm{D}$	$b/x = \mathrm{D}^*$	$\gamma b/x$	$\boldsymbol{U}$	$\boldsymbol{u}$	$\boldsymbol{C}$	$\boldsymbol{c}$	R	S_1	$S_2 = \beta$	γ
Jirka [7]	0.156	0.175	0.17	3.63	2.96	3.63	3.49	1.00	1.38	1.22	0.96
Lee, Chu [6]	0.161	0.182	0.17	3.50	2.87	3.51	3.36	1.00	1.38	1.22	0.96
Hossain, Rodi [39]	0.146	0.179	0.13	3.50	3.10	4.29	3.19	0.83	1.39	1.13	0.74
Fisher et al. [11]	0.151	0.169	0.13	3.50	3.52	3.97	3.17	0.82	1.11	0.99	0.80
Min/Max	0.904	0.928		0.97	0.81	0.82	0.91				

Plume Author	$B/x = \mathrm{D}$	$b/x = \mathrm{D}^*$	$\gamma b/x$	$\boldsymbol{U}$	$\boldsymbol{u}$	$\boldsymbol{C}$	$\boldsymbol{c}$	R	S_1	$S_2 = \beta$	γ	$\frac{\Delta B}{U^2}$	$\frac{g' b}{u^2}$
Jirka [7]	0.14	0.160	0.15	2.45	2.01	6.56	6.29	1.00	1.38	1.22	0.96	0.15	0.25
Lee, Chu [6]	0.148	0.166	0.16	2.36	1.95	6.13	5.92	1.00	1.35	1.21	0.97	0.16	0.26
Hossain, Rodi [39]	0.191	0.167	0.23	1.90	1.84	4.61	6.21	1.11	0.90	1.03	1.35	0.25	0.31
Fisher et al. [11]	0.141	0.160	0.12	2.35	2.43	6.77	5.15	0.79	1.09	0.97	0.76	0.17	0.14
Min/Max	0.741	0.956		0.77	0.76	0.68	0.82						

Table 3 Weak jets in co-flow ($u_e \ll u_a$)

Plane jets, Jirka [12]										
$\frac{b_g u_a}{(2m_{oe}x)^{1/2}}$	λ	$\frac{u_{em}x^{1/2}}{(2m_{oe})^{1/2}}$	$\frac{c_m(2m_{oe}x)^{1/2}}{2c_0q_0}$	D	D*	γD*	R	S_1	β_e	γ
0.291[b]	1.3	1.94	1.49	0.133	0.180	0.18	1	1.17	1.16	0.99
Axisymmetric jets, Jirka [7]										
$\frac{b_g u_a^{2/3}}{(M_{oe}x)^{1/3}}$	λ	$\frac{u_e m x^{2/3}}{(M_{oe}u_a)^{1/3}}$	$\frac{c_m(M_{0e}x)^{2/3}}{u_a^{1/3}c_0Q_0}$	D	D*	γD*	R	S_1	β_e	γ
0.37	1.2	2.27	1.58	0.154	0.211	0.20	1	1.13	1.22	0.96

[b] From the entrainment coefficient

recommendations by Fisher et al. [11] for plane plumes lead to a value of $R = 0.65$, which is quite low. The width of jets and plumes determined from dye visualizations was found to agree well with h.

Table 1 shows that at least according to the two recent recommendations γ is close to one, i.e. the entraining interface at γh coincides quite well with the boundary of excess mass or tracer at h. This indicates that the ratio $hu/q_0 = g_0'/g'$ agrees with the dilution $\gamma hu/q_0$, and suggests that mass-based scales derived from the flux and distribution a passive tracer can also be used for free shear flows in stratified ambient fluids by expressing (19) in terms of the concentration of that tracer. Similar considerations apply for axisymmetric flows in Table 2. The determination of the volume flux, and of γ, is particularly difficult for axisymmetric jets, as errors due to induced ambient flows can be large near the boundaries. The sensitivity to such errors can also be illustrated by computing the flux for a given half-width b_u and a velocity u_m for different velocity profiles. For the algebraic profile function based on a constant eddy viscosity (see Schlichting [2]), the flux is 67% larger than for a Gaussian, even though this author claims good agreement with the velocity measurements. Conversely, the momentum flux is only 12% larger, as the small velocities near the boundary are squared.

A hopeful feature of the last row (Min/Max) in Tables 1 and 2 is that the discrepancy of the mass-based widening rates D* is smaller than that of the velocity-based rates D. This also holds for the nondimensional concentrations $\boldsymbol{c}$ and $\boldsymbol{C}$, but not for the velocities $\boldsymbol{u}$ and $\boldsymbol{U}$ in plane jets and axisymmetric flows. Considering that it is not clear how well the Gaussian distribution represents the concentration profiles in different flows, the widening rates D* also agree rather well with the value of $\tilde{b}/x = 0.17$ based on the integral over the intermittency distribution, which Chu [10] found to be quite universal for free shear flows.

For jets in co-flows the excess velocity is small in a region far from the source, and the shape factor S_2 is equal 1. The corresponding recommendations of Jirka [7,12] are shown in Table 3. As his values of λ are the same for jets in co-flows as for those in calm ambients, the ratios of U/u_{em}, u_e/u_{em}, B/b_g, b/b_g, and c/c_m also remain the same.

The table shows that the values of D and D* agree fairly well with those in calm ambients, considering again that the velocity and buoyancy profiles may be slightly different.

6 Conclusions

In a first part of this study the diffusion model of Prandtl for the widening rate *DH/DT* of free shear flows is compared with the entrainment concept, which was developed for a depth-averaged description of such flows. The difference is that the widening rate of the

flow only depends on the streamwise excess velocity, whereas the entrainment rate *Eu* of ambient fluid also depends on the streamwise velocity gradient. It is shown that the area of the contorted turbulent/nonturbulent interface of such flows also depends on the streamwise gradient. The entrainment and diffusion concepts agree for uniform gravity currents ($\mathrm{d}U/\mathrm{d}x = 0$). Experimental data for wall jets and wall plumes indicate that the diffusion relation is the one appropriate for strongly entraining supercritical gravity currents, which are similar to free shear flows. For subcritical currents the entrainment and diffusion functions are identical even when the flow is not uniform. The diffusion function D thus describes the entrainment-induced depth change over the entire range of gravity currents.

ET's depth-averaged flow scales for gravity currents were derived from the velocity distribution, in analogy to those of MTT. Depth-averaged scales are also used for open channel flows, but they are derived from the depth, and the flux, of the liquid phase. To use the same scales for both types of flows we extended the ones for open channel flows to gravity currents in a previous contribution. In the present study they are extended further to free shear flows. In our view the concept of mass-based flow scales could provide a solid basis for future work on depth-averaged models of gravity currents and free shear flows. The main reason for our expectation is that are they, and the corresponding shape factors, are consistent with those of open channel flows. Furthermore, mass-based scales are easily determinable, suitable in the presence of co-flows, and the average concentration of a pollutant in the flow depends on the concentration distribution instead of the velocity distribution.

To provide first data we determined mass-based flow scales for free shear flows from available experimental data. The results for plane and axisymmetric jets and plumes suggest that the top-hat boundaries of excess motion and excess mass (or tracer) coincide ($\gamma \sim 1$), which would make mass-based scales suitable for describing free shear flows in a stratified environment. The momentum coefficient β is in the same range as for open channel and ducted flows, and the flow parameters recommended by different investigators are more consistent with each other when expressed in terms of mass-based than in terms of velocity-based flow scales.

References

1. Prandtl L (1926) Ueber die ausgebildete Turbulenz. In: Proceedings of the 2nd international congress for applied mechanics, Zurich, Sep 12–17, pp 62–74
2. Schlichting H (1979) Boundary layer theory. 7. McGraw Hill, New York
3. Abramovich GN (1963) The theory of turbulent jets. MIT Press, Cambridge
4. Morton BR, Taylor GI, Turner JS (1956) Turbulent gravitational convection from maintained and instantaneous sources. Proc R Soc Lond A 234:1–23
5. List EJ, Imberger J (1973) Turbulent entrainment in buoyant jets. J Hydraul Div ASCE 99:1461–1474
6. Lee JHW, Chu VH (2003) Turbulent jets and plumes: a Lagrangian approach. Kluwer, Dordrecht
7. Jirka GH (2004) Integral model for turbulent buoyant jets in unbounded stratified flows, Part 1. The single round jet. Environ Fluid Mech 4:1–56
8. Bühler J, Papantoniou DA (2001) On the motion of suspension thermals and particle swarms. J Hydraul Res 39(6):643–653
9. Patel RP (1971) Turbulent jets and wall jets in uniform streaming flow. Aeronaut Q XXII:311–326
10. Chu VH (1994) Lagrangian scaling of turbulent jets and plumes with dominant eddies. In: Davies PA, Nieves V (eds) Recent research advances in the fluid mechanics of turbulent jets and plumes. NATO ASI Series. Kluwer, Dordrecht pp 45–72
11. Fischer HB, List EJ, Koh RCY, Imberger J, Brooks NH (1979) Mixing in inland and coastal waters. Academic Press, New York
12. Jirka GH (2006) Integral model for turbulent buoyant jets in unbounded stratified flows, Part 2: plane jet dynamics resulting from multiple port diffuser jets. Env Fluid Mech 6:43–100
13. Ellison TH, Turner JS (1959) Turbulent entrainment in stratified flows. J Fluid Mech 6:423–448

14. Parker G, Garcia M, Fukushima Y, Yu W (1987) Experiments on turbidity currents over an erodible bed. J Hydraul Res 25(1):123–146
15. Alavian V, Jirka GH, Denton RA, Johnson MC, Stefan HG (1992) Density currents entering lakes and reservoirs. J Hydraul Eng 118(11):1464–1489
16. Altinakar MS (1993) Weakly depositing turbidity currents on small slopes. PhD thesis Nr. 738, Department of Civil Engineering, Ecole Polytechnique Fédérale de Lausanne (EPFL), Lausanne, Switzerland
17. Fernandez RL, Imberger J (2006) Bed roughness induced entrainment in a high Richardson number underflow. J Hydraul Res 44(6):725–738
18. Manins PC, Sawford BL (1979) A model of katabatic winds. J Atmos Sci 36:619–630
19. Legg S, Brieglieb B, Chang Y et al (2009) Improving oceanic overflow representation in climate models. Bull Am Meteorol Soc 90(5):657–670
20. Oehy CD, De Cesare G, Schleiss AJ (2010) Effect of inclined jet screen on turbidity current. J Hydraul Res (accepted for publication)
21. Chow V-T (1959) Open channel hydraulics. McGraw Hill, New York
22. Bühler J, Siegenthaler C (1986) Self-preserving solutions for turbidity currents. Acta Mech 63(11):217–233
23. Princevac M, Bühler J, Schleiss AJ (2009) Mass-based depth and velocity scales for gravity currents and related flows. Environ Fluid Mech 9:369–387
24. Prandtl L (1942) Bemerkungen zur Theorie der freien Turbulenz. Z Angew Math Phys (ZAMP) 22(5):241–253
25. Hunt JCR, Eames I., Westerweel J (2006) Mechanics of inhomogeneous turbulence and interfacial layers. J Fluid Mech 554:499–519
26. Gaskin S, Wood IR (2001) The axisymmetric and the plane jet in a coflow. J Hydraul Res 39(4):1–8
27. Turner JS (1986) Turbulent entrainment: the development of the entrainment assumption, and its application to geophysical flows. J Fluid Mech 173:431–471
28. Holzner M, Liberzon A., Nikitin N, Lüthi B, Kinzelbach W, Tsinober A (2008) A Lagrangian investigation of the small scale features of turbulent entrainment through 3D-PTV and DNS. J Fluid Mech 598:465–475
29. Mathew J, Basu AJ (2002) Some characteristics of entrainment at a cylindrical turbulence boundary. Phys Fluids 14(7):2065–2072
30. Holzner M, Lüthi B, Liberzon A, Tsinober A, Kinzelbach W (2009) The local entrainment velocity is a viscous quantity. In: Hanjali K, Nagano Y, Jakirli S (eds) Proceedings of the 6th conference on turbulence, heat and mass transfer, September 14–18. Rome, pp 77–80
31. Townsend AA (1956) The structure of turbulent shear flow. Cambridge University Press, London
32. Grella JJ, Faeth GM (1975) Measurements in a two-dimensional thermal plume along a vertical adiabatic wall. J Fluid Mech 71(4):701–710
33. Odier O, Chen J, Rivera MK, Ecke RE (2009) Mixing in stratified gravity currents: the Prandtl mixing length. Phys Rev Lett 102(13):Art. No. 134504
34. Bühler J, Wright SJ, Kim Y (1991) Gravity currents advancing into a coflowing fluid. J Hydraul Res 29(2):243–257
35. Princevac M, Fernando HJS, Whiteman D (2005) Turbulent entrainment into natural gravity-driven flows. J Fluid Mech 533:259–268
36. Noh Y, Fernando HJS (1991) Gravity current propagation along an incline in the presence of boundary mixing. J Geophys Res 96(C7):12586–12592
37. Scheepbouwer E, Davidson MJ, Nokes RI (2008) Tracer distribution of line advected thermals. Environ Fluid Mech 8:561–568
38. Wright SJ (1994) The effect of ambient turbulence on jet mixing. In: Recent research advances in the fluid mechanics of turbulent jets and plumes. NATO ASI Series. Kluwer, Dordrecht, pp 13–27
39. Hossain MS, Rodi W (1982) A turbulence model for buoyant flows and its application to vertical buoyant jets. In: Rodi W (ed) Turbulent buoyant jets and plumes. HMT Series, vol 6. Pergamon Press, New York, pp 121–178